Neuroscience Research 64 (2009) 41–49

Contents lists available at ScienceDirect

Neuroscience Research

journal homepage: www.elsevier.com/locate/neures

Characterisation of human mesenchymal stem cells following differentiation into Schwann cell-like cells

Maria Brohlin [a,1], Daljeet Mahay [b,1], Lev N. Novikov [a], Giorgio Terenghi [b], Mikael Wiberg [a,c], Susan G. Shawcross [b], Liudmila N. Novikova [a,*]

[a] Department of Integrative Medical Biology, Section of Anatomy, Umeå University, SE-901 87 Umeå, Sweden
[b] Blond McIndoe Research Laboratories, Tissue Injury and Repair Group, The University of Manchester, 3.106 Stopford Building, Oxford Road, Manchester M13 9PT, UK
[c] Department of Surgical and Perioperative Science, Section of Hand and Plastic Surgery, Umeå University, SE-901 87 Umeå, Sweden

ARTICLE INFO

Article history:
Received 7 October 2008
Received in revised form 7 January 2009
Accepted 16 January 2009
Available online 30 January 2009

Keywords:
Bone marrow stromal cell
Schwann cell
Glial cell
Differentiation
Dorsal root ganglion
Glial growth factor

ABSTRACT

Cell-based therapies provide a clinically applicable and available alternative to nerve autografts. Our previous studies have characterised rat-derived mesenchymal stem cells (MSC) and here we have investigated the phenotypic, molecular and functional characteristics of human-derived MSC (hMSC) differentiated along a Schwann cell lineage. The hMSC were isolated from healthy human donors and the identity of the undifferentiated hMSC was confirmed by the detection of MSC specific cells surface markers. The hMSC were differentiated along a glial cell lineage using an established cocktail of growth factors including glial growth factor-2. Following differentiation, the hMSC expressed the key Schwann cell (SC) markers at both the transcriptional and translational level. More importantly, we show the functional effect of hMSC on neurite outgrowth using an *in vitro* co-culture model system with rat-derived primary sensory neurons. The number of DRG sprouting neurites was significantly enhanced in the presence of differentiated hMSC; neurite length and density (branching) were also increased. These results provide evidence that hMSC can undergo molecular, morphological and functional changes to adopt a SC-like behaviour and, therefore, could be suitable as SC substitutes for nerve repair in clinical applications.

1. Introduction

Peripheral nerve injuries are an economic burden for society in general and despite advanced microsurgical reconstruction of the damaged nerves the functional result is unsatisfactory with poor sensory recovery and reduced motor functions (Wiberg and Terenghi, 2003). In the treatment of nerve injuries transplantation of a nerve graft is often necessary, especially in nerve gap injuries. More recently, promising functional results have been achieved using different types of conduits containing cultured Schwann cells (SCs) and *in vitro* differentiated bone marrow stromal cells with Schwann cell properties (Dezawa et al., 2001; Mosahebi et al., 2002; Keilhoff et al., 2006; Pfister et al., 2007; Shimizu et al., 2007). Schwann cells are the key facilitators of peripheral nerve regeneration and are responsible for the formation and maintenance of the myelin sheath around axons in peripheral nerve fibres. They are essential for nerve regeneration after nerve injuries as they produce extracellular matrix molecules, integrins and trophic factors providing guidance and trophic support for regenerating axons (Bunge, 1994; Ide, 1996; Mahanthappa et al., 1996; Terenghi, 1999; Wiberg and Terenghi, 2003). However, the use of *ex vivo* cultured SC within conduits is limited in its clinical application because of the concomitant donor site morbidity and the slow growth of these cells *in vitro* (Tohill et al., 2004).

Mesenchymal stem cells (MSC or bone marrow stromal cells) are easily accessible non-haematopoietic stem cells that have proved essential for research purposes due to their plasticity and ability to differentiate into several functional cell types. *In vitro*, they display a fibroblastic morphology and readily adhere to plastic surfaces (Pittenger et al., 1999; Krampera et al., 2007). By nature, these cells are a heterogeneous population, thus there is problem finding a specific marker that defines their origin. MSCs are CD14, CD34, CD45 negative and CD44, CD54, CD90 and Stro-1 positive (Barry, 2003; Bobis et al., 2006; Phinney, 2007).

* Corresponding author. Tel.: +46 90 786 5132; fax: +46 90 786 5480.
E-mail address: liudmila.novikova@anatomy.umu.se (L.N. Novikova).
[1] Joint first authors.

Abbreviations: αMEM, alpha modified Eagle's medium; dhMSC, differentiated human-derived mesenchymal stem cells; DMEM, Dulbecco's MEM; DRG, dorsal root ganglia; FACS, fluorescence activated cell sorting; FBS, foetal bovine serum; GFAP, glial fibrillary acidic protein; GGF-2, glial growth factor-2; hMSC, human-derived mesenchymal stem cells; MEM, modified Eagle's medium; MSC, mesenchymal stem cells; P, patient; PE, phycoerythrin; SC, Schwann cells; RT-PCR, reverse transcriptase polymerase chain reaction; uhMSC, undifferentiated human-derived mesenchymal stem cells.

0168-0102/$ – see front matter © 2009 Elsevier Ireland Ltd and the Japan Neuroscience Society. All rights reserved.
doi:10.1016/j.neures.2009.01.010

Studies by our group and others have shown that following differentiation with a cocktail of growth factors, MSCs express glial cell markers, such as glial fibrillary protein (GFAP), low-affinity neutrophin factor p75 and calcium binding protein S100 (Dezawa et al., 2001; Tohill et al., 2004; Caddick et al., 2006; Zurita et al., 2007; Lin et al., 2008). Clearly, it is of considerable clinical importance to establish the differentiation of human-derived MSC (hMSC) into SC-like cells (dhMSC). This alternative source of cells, which is relatively simple to isolate and expand in culture, should provide nerve fibre support and guidance during nerve regeneration. Shimizu et al. (2007) have examined the clinical potential of SC-like cells in a rat sciatic nerve injury model. They have demonstrated that MSCs express SC markers *in vivo* and also come in close physical contact with the regenerating axons.

The purpose of this study is to identify the phenotypic, molecular and functional characteristics of hMSC differentiated into cells with a SC-like phenotype. We also assessed the function of the dhMSC as SC substitutes in a functional co-culture assay with dissociated rat primary sensory neurons. From a clinical standpoint, it is also important to assess the effects of patient age and gender on efficacy of hMSC as SC substitutes.

2. Materials and methods

2.1. Culture of bone marrow stromal cells

Samples of human bone marrow were obtained from the iliac crests of three healthy donors during reconstructive surgery with informed consent. The patients were designated as follows: P1 female aged 59 years, P2 male aged 58 years and P3 male aged 32 years. Procedures were approved by the Local Ethical Committee for Clinical Research in Umeå University (no. 03-425).

A modification of previously described protocol (Azizi et al., 1998) was used to isolate and to prepare primary cultures of hMSC. Briefly, bone marrow samples were rinsed thoroughly with alpha modified Eagle's medium (αMEM) containing 10% (v/v) foetal bovine serum (FBS), 1% (v/v) penicillin–streptomycin (all Invitrogen Life Technologies, Paisley, UK). The cell suspension was centrifuged at 1500 × *g* for 5 min and the cell pellet was filtered through a 70-μm nylon mesh (BD Falcon, Becton, Dickinson and Company, Oxford, UK), plated in 75 cm^2 tissue culture flasks (Corning, USA) and incubated at 37 °C, 5% (v/v) CO_2. After 24 h in culture, the supernatant containing non-adherent cells was removed and discarded and fresh medium added. The cells attached to the culture flask were cultured at 37 °C, 5% CO_2 for 2–3 weeks with medium changes every 48 h. When the cultures had reached 80% confluence, the cells were enzymatically detached from the flask using 1.25% trypsin/EDTA solution (Invitrogen Life Technologies) and re-seeded in new culture flasks at a density of 5×10^3 cells cm^{-2}.

2.2. Characterisation of bone marrow stromal cells

The isolation of MSC was based upon their ability to adhere to plastic surfaces (Azizi et al., 1998; Hofstetter et al., 2002). To confirm the multipotency of the hMSC, the cultures were differentiated into osteoblasts, chondrocytes or adipocytes according to the previously published protocols (Pittenger et al., 1999; Caddick et al., 2006; Mahay et al., 2008a). The cultures were treated for 3 weeks with the different induction media. Osteogenic induction medium comprised 10 mM β-glycerophosphate, 0.1 μM dexamethasone and 100 μg ml^{-1} ascorbate (all Sigma–Aldrich) in αMEM (Invitrogen). Chondrogenic induction medium was prepared from 0.01 nM dexamethasone, 50 μg ml^{-1} ascorbate, 40 μg ml^{-1} proline, 10 ng ml^{-1} transforming growth factor β1 (all Sigma–Aldrich) and 1% ITS-Plus (BD Falcon) in high glucose Dulbecco's MEM (DMEM, Invitrogen). Adipogenic induction medium contained 1 μM dexamethasone, 10 μg ml^{-1} insulin and 3-isobutyl-1-methylxantine (all Sigma–Aldrich) in high glucose DMEM. After the differentiation processes were complete, the cultures were fixed with 4% paraformaldehyde in 0.1 M phosphate buffer (pH 7.4) and stained for osteoblasts, chondrocytes and adiopocytes using Alizarin red, Toluidine Blue and Oil Red O, respectively (all Sigma–Aldrich).

2.3. Differentiation into Schwann-like cells

The differentiation process was initiated in sub-confluent hMSC cultures at the second passage by replacing growth medium with αMEM containing 1 mM beta-mercaptoethanol (Sigma–Aldrich) for 24 h. Cells were then incubated for 72 h with growth medium containing 35 ng ml^{-1} all-*trans*-retinoic acid (Sigma–Aldrich) followed by growth medium supplemented with 5.7 μg ml^{-1} forskolin (MP Biomedicals, Sweden), 10 ng ml^{-1} basic fibroblast growth factor (Invitrogen), 5 ng ml^{-1} platelet-derived growth factor-AA (Millipore) and 126 ng ml^{-1} glial growth factor-2 (GGF-2, Acorda Therapeutics Inc., USA). The cells were maintained in this supplemented medium for 2 weeks with medium changes every 72 h to establish differentiated cultures (Dezawa et al., 2001; Tohill et al., 2004; Caddick et al., 2006).

2.4. Immunocytochemistry for MSC and Schwann cell markers

Cells were subcultured at 37 °C with 5% CO_2 on slide flasks (Nunc, Fisher Scientifics, Loughborough, UK) at a density of 15×10^3 cells per flask for 2 days. The cells were fixed with 4% paraformaldehyde in 0.1 M phosphate buffer (pH 7.4) for 20 min and the flasks were detached from the slides. After blocking with normal goat serum, cells were incubated overnight at 4 °C with mouse monoclonal antibodies against CD14 (1:1000; Millipore), CD45 (1:200; Millipore), CD54 (1:75; Millipore), CD90 (1:50; Serotec), Stro-1 (1:50; R&D Systems) and rabbit polyclonal antibodies against S100 protein (1:500; Dako) and low-affinity NGF p75 receptor (1:500; Promega). After rinsing in PBS, secondary goat anti-mouse antibodies Alexa Fluor® 488 and Alexa Fluor® 568 (1:1000; Invitrogen) or fluorescein isothiocyanate (FITC)-linked rabbit secondary antibody (Vector Laboratories Ltd., Peterborough, UK) were applied for 2 h at ambient temperature in the dark. The cells were mounted with Vectashield® (Vector Laboratories) or ProLong (Invitrogen) mounting mediums containing DAPI. The staining specificity was tested by omission of primary antibodies. Monocytes and granulocytes in the smears prepared from normal blood donor were used as positive controls for CD14 and CD45 immunostaining. Preparations were photographed with a Nikon DXM1200 digital camera attached to a Leitz Aristoplan microscope. The captured images were resized, grouped into a single canvas and labelled using Adobe Photoshop CS3 software. The contrast and brightness were adjusted to provide optimal clarity.

2.5. Fluorescence activated cell sorting (FACS)

The uhMSC were additionally identified by flow-cytometry using anti-human CD44 antibodies (Serotec). After detachment from the culture flasks, the cells were re-suspended in FACS buffer (PBS, pH 7.4 with 3% (v/v) FBS and 0.01% (w/v) sodium azide) and incubated with phycoerythrin (PE)-conjugated antibodies in the dark for 20 min on ice. Cells were washed once and re-suspended in a small volume of FACS buffer to achieve a concentration of $(2–5) \times 10^6$ cells ml^{-1}. The $CD44^+$ PE-labelled cells were detected using a FACSCalibur (DiVa, BD Biosciences, San Jose, USA) and analyzed with CellQuest Pro software.

2.6. RT-PCR for glial markers

The RNeasy™ mini kit (QIAGEN Ltd., UK) was used for the isolation of total RNA from the cell pellets of the uhMSC and dhMSC from the three patients as previously described (Mahay et al., 2008a) and using primers synthesised by Invitrogen (see Table 1). The optimum annealing temperature for each primer pair was determined experimentally. The One-Step RT-PCR kit (QIAGEN Ltd.) was used for all RT-PCRs as per the manufacturer's instructions with the addition of 1 ng total cellular RNA or RNase-free water (negative control). An MJ Research PTC-200 thermal cycler was used for all reactions. The cycling parameters were as follows: a reverse transcription step (50 °C, 30 min), a denaturation/reverse transcriptase inactivation step (95 °C, 15 min) followed by 35 cycles of denaturation (95 °C, 30 s), annealing (30 s, see Table 1) and primer extension (72 °C, 1 min) followed by final extension incubation (72 °C, 5 min).

Once the thermal cycling was complete, a qualitative assessment of the integrity and size of the resulting amplicons was done by electrophoresis (50 V, 90 min)

Table 1
Human oligonucleotide primers.

Human primers (Genbank accession codes)	Forward primer (5′–3′)	Reverse primer (5′–3′)	Annealing temp. (°C)
S100 (BC001766)	GGA AAT CAA AGA GCA GGA GGT	ATT AGC TAC AAC ACG GCT GGA	54.8
GFAP (NM_002055)	GTC CAT GTG GAG CTT GAC G	CAT TGA GCA GGT CCT GGT AC	60.7
P75 (NM_002507)	TGG ACA GCG TGA CGT TCT CC	GAT CTC CTC GCA CTC GGC GT	60.7 (Harada et al., 2002)
erbB3 (BC082992)	GGA GTC TTG CCA GGA GTC T	AGG AGT CAG CAG ACT GTG G	54.0 (Bovetti et al., 2006)[a]
GAPDH (XR_018781)	GAA GGT GAA GGT CGG AGT	CAA GCT TCC CGT TCT CAG C	63.2 (Tricarico et al., 2002)

[a] Sequence modified from source.

through a 2% (w/v) agarose gel (Melford Laboratories Ltd., UK) followed by straining with ethidium bromide (0.5 mg ml^{-1}, Sigma–Aldrich). The length (in base pairs) of the PCR products was estimated by comparison with DNA standards, Hyperladder IV (Bioline, UK). Images were captured using an AlphaImager 2200 (AlphaInnotech, USA) gel documentation system. The RT-PCR procedure was repeated ($n = 5$) for each of the six groups (uhMSC and dhMSC for P1–P3 patients). The nucleotide sequence of each amplicon was confirmed using the Big Dye™ Terminator sequencing kit (Applied BioSystems Incorporated, USA) and protocol followed by sequence analysis on the Prism 3100 Genetic Analyzer (Applied Biosystems Incorporated). It was necessary to use biphasic PCR methodology to detect the low-level transcripts of GFAP and erbB3. Following RT-PCR amplification (first round) of the GFAP and erbB3 transcripts, the reaction products were purified using a QiaQuick PCR clean-up (QIAGEN) and re-amplified using a standard PCR kit (Bioline, UK). The resulting products were subjected to agarose gel electrophoresis and DNA sequencing to verify their identity.

2.7. Western blotting of whole cell protein lysates

Whole cell lysates were prepared from cells cultured to confluence as previously described (Mahay et al., 2008a). Briefly, cell pellets were re-suspended in whole cell lysis buffer (100 mM PIPES, 5 mM $MgCl_2$, 5 mM EGTA, 20% (v/v) glycerol, 0.5% (v/v) Triton X-100 and 0.005% (v/v) protease inhibitor cocktail; all Sigma–Aldrich). Protein concentrations were determined using the DC protein assay system (Bio-Rad Laboratories, Hercules, CA, USA). Proteins were separated by denaturing (SDS) electrophoresis through 10% (w/v) acrylamide gels at 120 V using the Bio-Rad mini-Protean 3 (Bio-Rad laboratories). The separated proteins were transferred onto nitrocellulose membranes using the Bio-rad transblot system (Bio-Rad laboratories) (30 V, 90 min). The membranes were incubated (4 °C overnight) with anti-S100 (rabbit polyclonal; 1:500, Dako, Denmark), anti-GFAP (mouse monoclonal; 1:200, Stratech Scientific Ltd., UK), anti-p75 (rabbit polyclonal; 1:300, Promega, UK) or anti-erbB3 (mouse monoclonal; 1:200; Santa Cruz) antibodies. Additionally, beta tubulin antibody (rabbit polyclonal; 1:2000; Abcam, ab6046, Cambridge, UK) was used as a loading control. The membranes were incubated (21 °C, 1 h) with HRP-conjugated secondary antibodies (horse anti-mouse at 1:1000 or horse anti-rabbit at 1:2000) and treated with ECL chemiluminescent HRP substrate (Amersham Biosciences, UK). The membranes were subjected to autoradiography by exposure to Kodak X-OMAT light-sensitive film.

2.8. Dorsal root ganglia co-culture

Dorsal root ganglia (DRG) were harvested from the spinal cords of adult male Sprague–Dawley rats using a previously described protocol (Caddick et al., 2006; Mahay et al., 2008b). Dissociated neurons were re-suspended in modified Bottenstein and Sato's medium (F12 medium containing 100 μM putrescine, 30 nM sodium selenite, 20 nM progesterone, 1 mg ml^{-1} bovine serum albumin, 0.1 mg ml^{-1} transferrin, 0.01 mM cytosine arabinoside and 10 pM insulin; all Sigma–Aldrich). The DRG neurons were seeded onto laminin-coated glass cover slips (Sigma–Aldrich) inserted into six-well plates and incubated for 24 h (37 °C, 5% CO_2).

24 h prior to DRG harvest, cultures of uhMSC and dhMSC from the three patients were seeded onto 1.0 μm pore size polyethylene terephthalate membrane cell culture inserts (BD Falcon) at a density of 150,000 cells in 2 ml/insert and incubated for 48 h (37 °C, 5% CO_2). The inserts were checked for cell adherence then placed into wells containing DRG neurons to establish the co-culture; these were allowed to incubate for 24 h (37 °C, 5% CO_2). Additional controls with the cell-free inserts were also analyzed (data not showed).

After 24 h in culture, the cells on the cover slips in the six-well plate were fixed in 4% (w/v) paraformaldehyde (20 min, 4 °C) and immunostained for anti-βIII tubulin (monoclonal, 1:1000, Sigma–Aldrich) with secondary antibodies Cy3-conjugated goat anti-mouse (1:100, GE Healthcare, UK). The cover slips were mounted with Vectashield™ (Vector Labs) and examined using a fluorescence microscope (Olympus BX60). The images were captured for quantification at 10× magnification using an Evolution QEi monochrome digital camera (Media Cybernetics, USA); image analysis was done using Image-Pro Plus Imaging software (Media Cybernetics, USA). Additional immunocytochemical stain with no primary antibody was carried out as a control.

2.9. Neurite outgrowth analysis

Neurite outgrowth was assessed using three independent parameters: percentage of process-bearing neurons, length of longest neurite and total neurite density (total no. of intersection points of a concentric circle set with radii increasing by 33 μm) using the previously described SigmaScan Pro 5 software macro (Caddick et al., 2006; Mahay et al., 2008b). Four independent co-culture experiments were carried out and neurite outgrowth assessed.

2.10. Cell proliferation assay

The CellTiter 96® AQueous One Solution Cell Proliferation Assay kit (Promega, Southampton, UK) was used for detection of cells proliferation. Briefly, hMSC cultures were trypsinized and seeded into 96-well culture plates (5×10^3 cells in 100 μl of growth medium per well with five replicates per culture). After 2 h, the old media was removed and 100 μl of fresh media was added to each well and 20 μl of 3-(4,5-dimethylthiazol-2-yl)-5-(3-carboxymethoxyphenyl)-2-(4-sulphophenyl)-2H-tetrazolium, inner salt and an electron coupling reagent, phenazine methosulphate solution per well was added and cultures were maintained at 37 °C, 5% CO_2 for 2 h. The optical density of resulting formazan production was measured at 490 nm using a Spectra Max 190 microplate reader (Molecular Device, Albertville, MN, USA). Optical density measurements were taken every day at the same time point for 3 consecutive days.

2.11. Statistical analysis

Statistical analysis was conducted using GraphPad Prism software (GraphPad Software Inc., USA). The data from the proliferation assays are expressed as

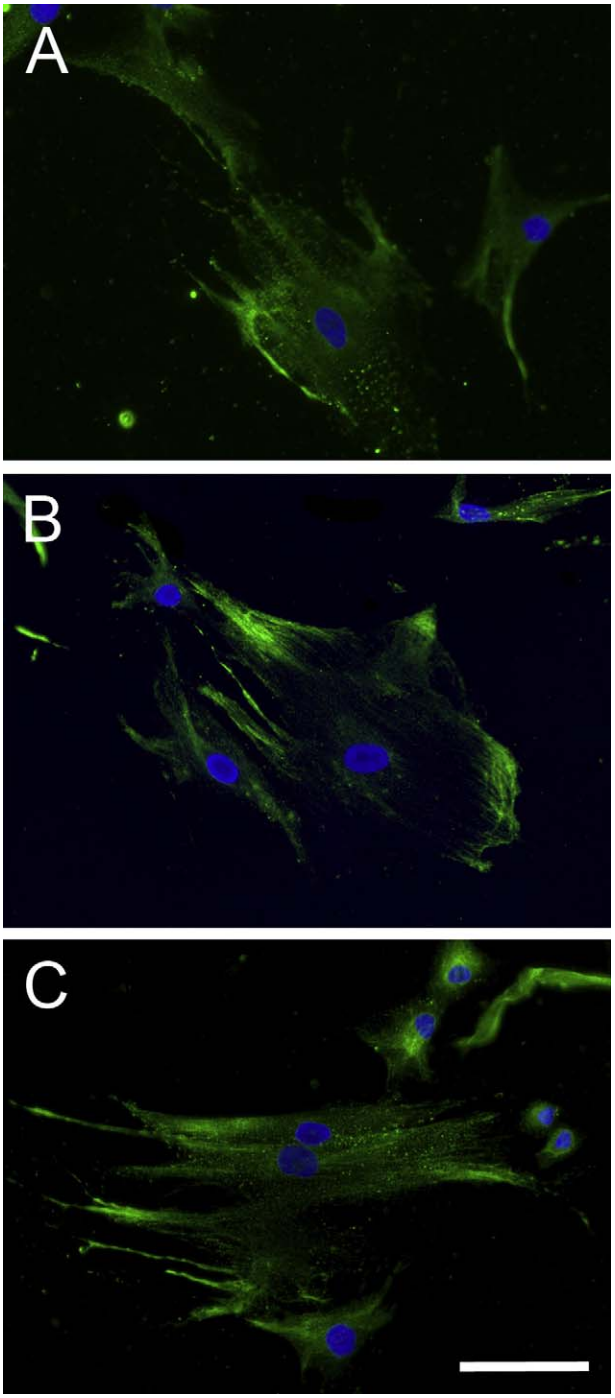

Fig. 1. Identification of stro-1 in hMSC. Immunocytochemical staining of cultured uhMSC from three patients, P1 (A), P2 (B) and P3 (C) for the MSC marker, stro-1 (FITC: green, DAPI: blue). Scale bar, 100 μm (A–C).

mean ± standard error of the mean (S.E.M.) following the *post hoc* Newman–Keuls multiple comparison test. The data for neurite outgrowth quantification are expressed as mean ± S.E.M. following one-way ANOVA followed by Bonferroni's multiple comparison test.

3. Results

3.1. Identification of MSC markers

Immunocytochemical labelling of the uhMSC showed positive staining for Stro-1 in 80% uhMSC of the three patients (Fig. 1). Staining for haemopoietic stem cell surface markers CD14 (Fig. 2A, E and I) and CD45 (Fig. 2B, F and J) was negative in the uhMSC of all three patients (P1–P3). More than 80% of uhMSC were positive for MSC surface markers CD54 (Fig. 2C, G and K) and CD90 (Fig. 2D, H and L). Flow-cytometry showed that approximately 40% of the uhMSC from each of the three patients expressed CD44. In a 2×10^6 aliquot (1 ml) of cells from each patient, 8.2×10^5 P1 cells were $CD44^+$ cells, 8.0×10^5 P2 cells were $CD44^+$ and 8.4×10^5 P3 cells were $CD44^+$ (Fig. 3).

3.2. Demonstration of the multilineage potential of hMSC

The multipotency of uhMSC from the three patients, P1 (Fig. 4A–C), P2 (Fig. 4D–F) and P3 (Fig. 4G–I), was demonstrated by their ability to differentiate into chondrocytes, osteoblasts and adipocytes in appropriate culture conditions. The sulphated proteoglycan of chrondrocytes was stained blue with Toluidine Blue (Fig. 4A, D and G), areas of calcification around osteoblasts were labelled red with Alizarin red (Fig. 4B, E and H) and the lipid droplets in the adipocytes were stained red with Oil Red (Fig. 4C, F and I).

3.3. Immunocytochemistry for glial markers in hMSC

Cultured uhMSC readily adhered to plastic surface and the majority of the cells in primary cultures from all three patients displayed a flattened fibroblast-like morphology. During growth factor-induced differentiation, uMSC changed their shape from flat to spindle-like morphology. The expression of the glial marker proteins confirmed by immunocytochemical staining showed positive staining for S100 (Fig. 5) and low-affinity NGF receptor p75 (Fig. 5) in 80% of dhMSC from the three patients compared to the uhMSC which showed negative staining for each patient as shown by the DAPI counterstaining.

3.4. Glial marker transcript expression in hMSC

The presence of the glial cell marker gene transcripts was detected by RT-PCR methodology (Fig. 6). This showed that dhMSC express the transcripts for S100 (408 bp amplicon), p75 (371 bp amplicon) and GFAP (406 bp amplicon) compared to the uhMSC from the three patients. The dhMSC expressed the transcripts for erbB3 (238 bp amplicon) and there was also a low-level of detection. In the dhMSC, the transcript levels for the genes of interest were similar in all three patients, except for the slightly lower levels of S100B and p75 transcripts in P2 and P1, respectively. RT-PCR amplification

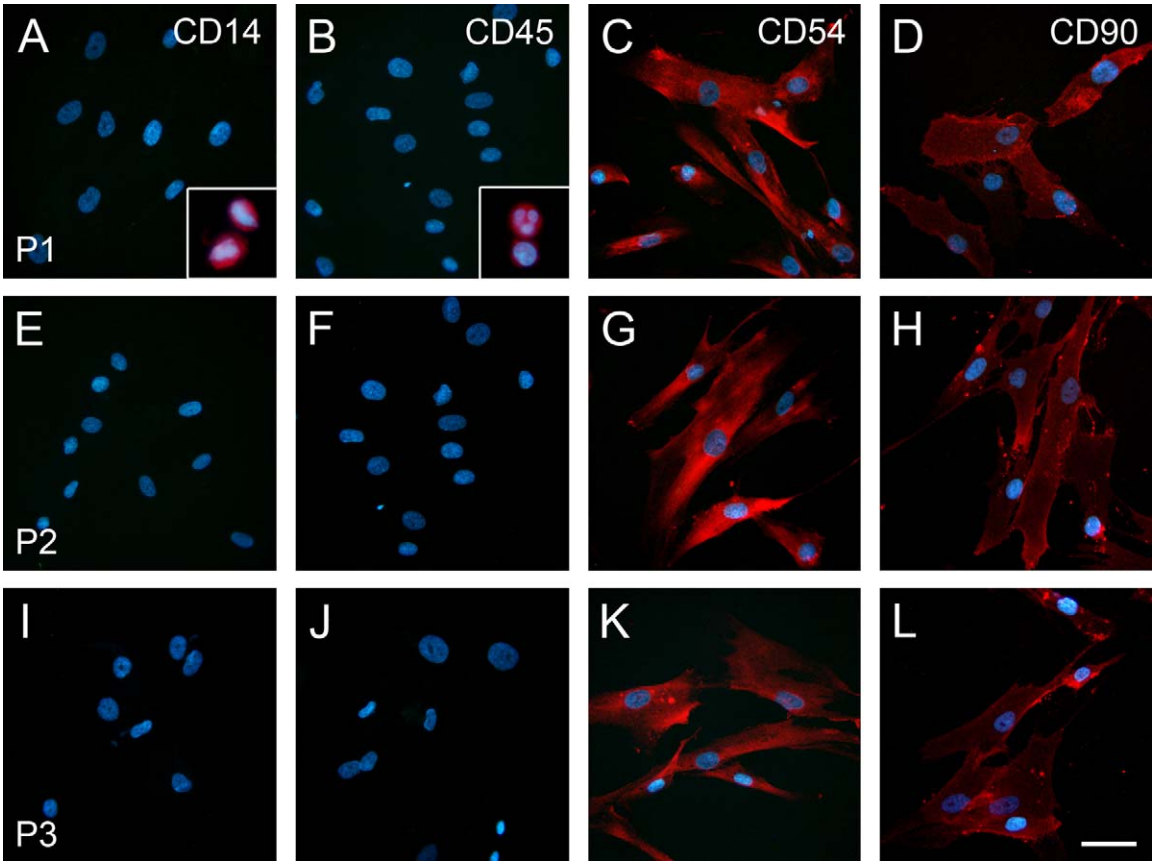

Fig. 2. Identification of MSC markers. Immunocytochemical staining (Cy3: red, DAPI: blue) of cultured uhMSC from three patients (P1–P3) for the haemopoietic cell surface markers CD14 (P1: A, P2: E, and P3: I) and CD45 (P1: B, P2: F, and P3: J) and MSC surface markers CD54 (P1: C, P2: G, and P3: K) and CD90 (P1: D, P2: H, and P3: L). Insertions in (A) and (B) are positive controls and show monocytes and granulocytes from normal blood donor smears immunostained for CD14 and CD45, respectively. Cell nuclei are counterstained with DAPI. Scale bar, 50 μm (A–L) and 20 μm (insertions in A and B).

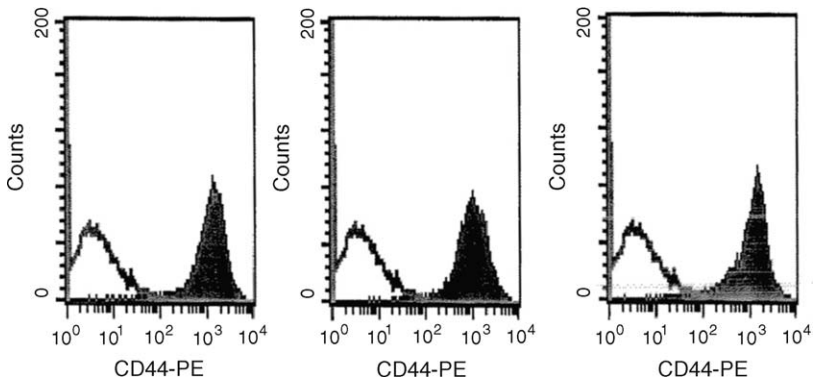

Fig. 3. FACS analysis for the MSC cell surface marker CD44 in uhMSC. Flow-cytometry traces from the sorting of 2×10^6 cells ml^{-1} using a PE-labelled CD44 antibody and FACSCalibur. Traces for $CD44^+$ uhMSC from patients P1–P3 show number of cells (*y*-axis) versus fluorescence intensity (*x*-axis).

efficacy of the mRNA was confirmed by the amplification of the constitutively expressed GAPDH (226 bp amplicon) housekeeping gene.

3.5. Expression of glial markers proteins in hMSC

Western blotting experiments (Fig. 7) showed that there was a higher level of protein expression for the glial proteins S100 (10 kDa), GFAP (51 kDa), p75 (75 kDa) and erbB3 (189 kDa) in dhMSC compared to uhMSC. In the dhMSC groups, the protein levels were similar in all three patients, except for slightly increased levels of GFAP in P1. The equivalence of total protein loading was confirmed using the constitutively expressed βIII tubulin (37 kDa) as a control.

3.6. DRG neurons co-culture functional bioassay with hMSC

Immunocytochemistical staining for βIII tubulin showed extensive neurite outgrowth by DRG neurons co-cultured with uhMSC from the three patients, P1 (Fig. 8A and B), P2 (Fig. 8C and D) and P3 (Fig. 8E and F). The neurite outgrowth by the DRG neurons was markedly enhanced in co-cultures with dhMSC (Fig. 8B, D and F) compared to the co-cultures with uhMSC (Fig. 8A, C and E) from the three patients.

These qualitative observations were confirmed by the quantification of three parameters of neurite growth: percentage DRG neurons sprouting neurites, length of longest neurite and neurite density. In all cases, the DRG co-cultured with dhMSC showed a statistically significant ($p < 0.01$ or $p < 0.001$) increase in neurite

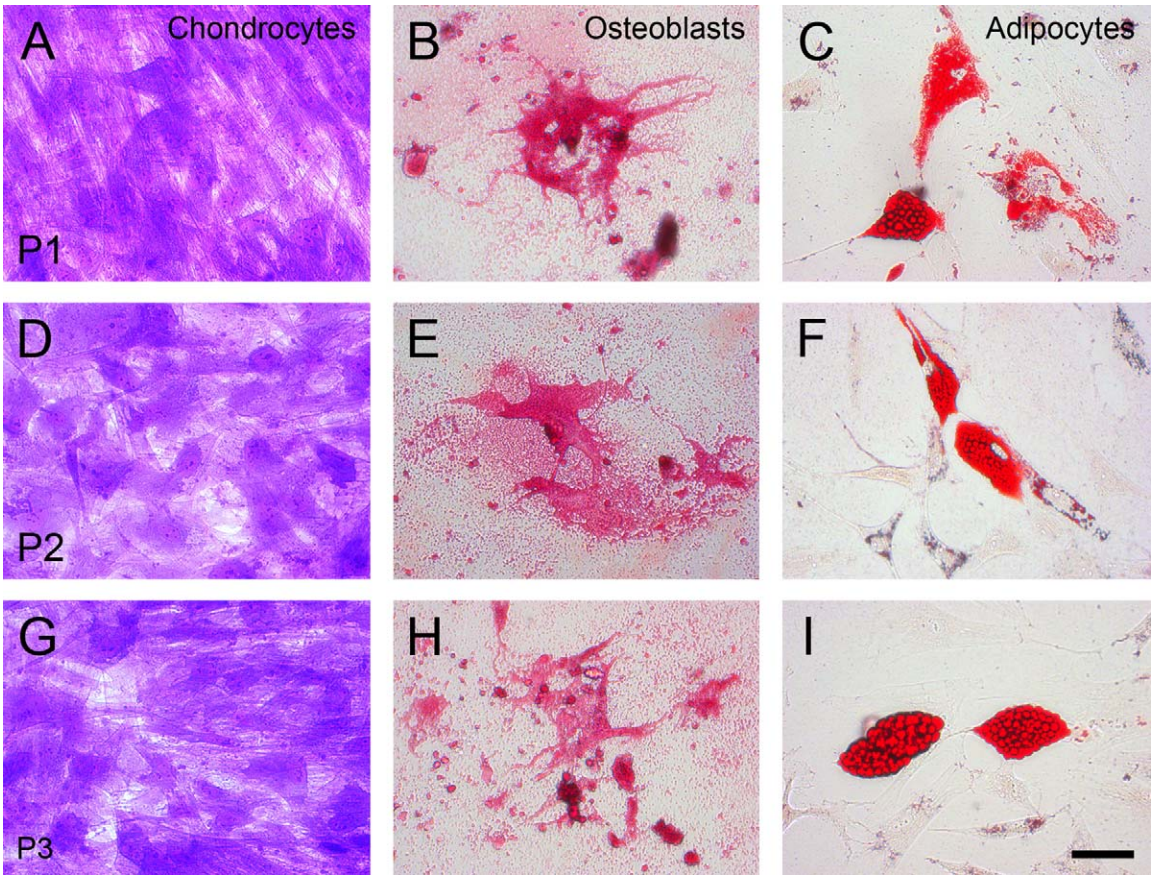

Fig. 4. Multilineage potential of hMSC. The hMSC from three patients (P1–P3) differentiated into chondrocytes (Toulidine blue staining: A, D and G), osteocytes (Alizarin red staining: B, E and H) and adipocytes (Oil Red staining: C, F and I). Scale bar, 50 μm (A–I).

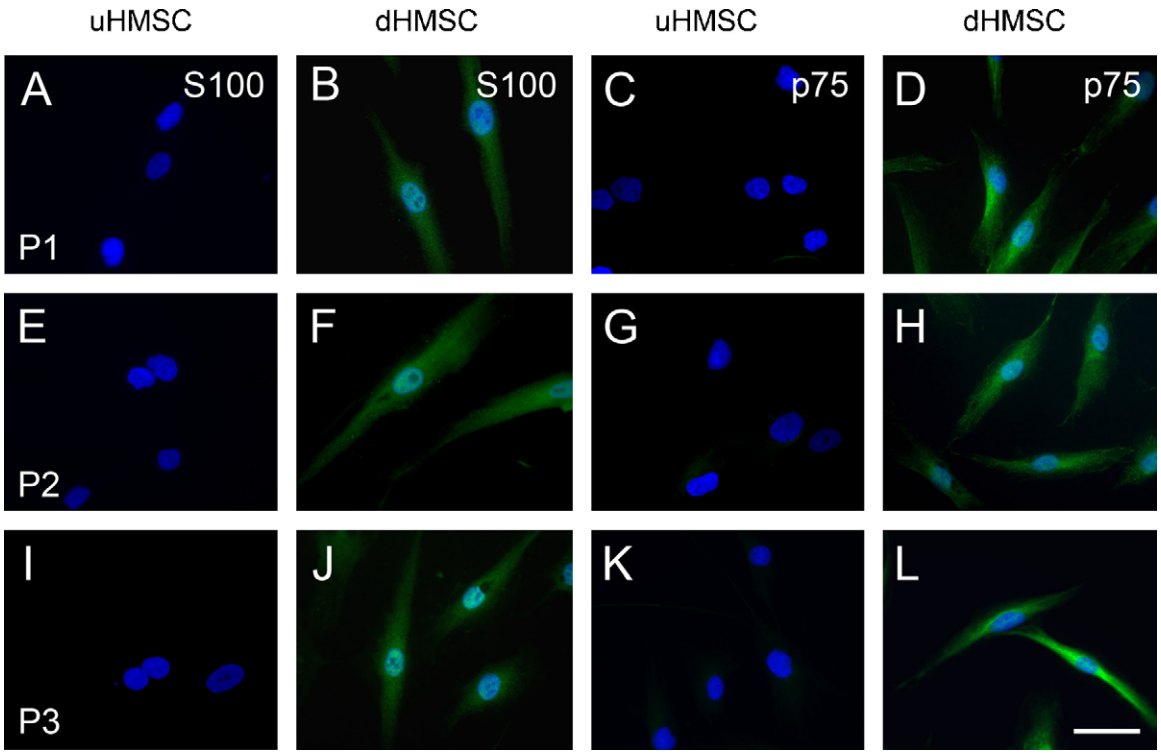

Fig. 5. Identification of Schwann cell markers in hMSC. Immunocytochemical staining of cultured hMSC from three patients, P1 (upper row), P2 (middle row) and P3 (lower row) for S100 protein in uhMSC (A, E, and I) and dhMSC (B, F, and J), and for low-affinity NGF p75 receptor in uhMSC (C, G, and K) and dhMSC (D, H, and L). Blue nuclei are stained with DAPI. Scale bar, 50 μm.

sprouting (Fig. 9A), neurite length (Fig. 9B) and total neurite density (Fig. 9C) compared to the co-cultures with uhMSC.

3.7. Comparison of proliferation rates of uhMSC and dhMSC

The proliferation rates of uhMSC and dhMSC from the three patients increased with time over a 72-h period (Fig. 10). As measure over a 72-h period, the differences in proliferation rates of the uhMSC and dhMSC for all three patients were statistically significant ($p < 0.001$; Fig. 10).

4. Discussion

In this study we have confirmed that the MSC from three healthy human donors express characteristic MSC cell surface markers and also demonstrated the multilineage potential of MSC (Pittenger et al., 1999; Krampera et al., 2007). Clear evidence is provided to show that human-derived MSC have the ability to differentiate along a glial lineage and express cell markers which are typical for glial cells including Schwann cells. Similar results have previously been reported for rat MSC (Tohill et al., 2004; Caddick et al., 2006; Zurita et al., 2007, 2008; Mahay et al., 2008a). An extensive characterisation of hMSC is essential before they can be considered as a potential clinical substitute for SC in peripheral nerve repair. Our results show that in a co-culture assay of DRG neurite outgrowth the performance of dhMSC is functionally analogous to SC (Caddick et al., 2006). This observation indicates that although there have been no genetic changes to these cells (e.g., introduction of extraneous genetic material), the phenotypic changes corre-

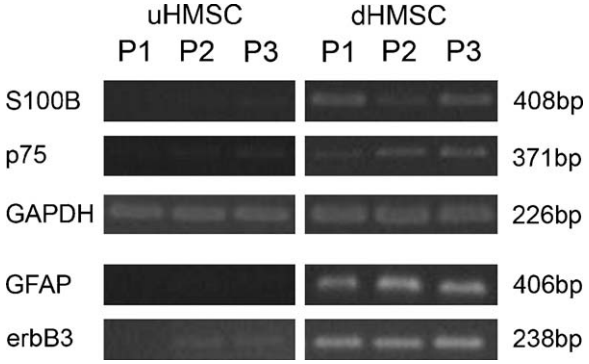

Fig. 6. Expression of glial marker transcripts in hMSC. RT-PCR for the assessment of transcript level of the glial cells markers S100B and p75 (A; amplification 1×), GFAP and erbB3 (B; amplification 2× or biphasic PCR) and the constitutively expressed housekeeping gene GAPDH in hMSC from three patients, P1–P3. Estimated amplicon lengths are shown in base pairs (bp). Biphasic PCR was used to increase assay sensitivity for the low-level transcripts of GFAP and erbB3.

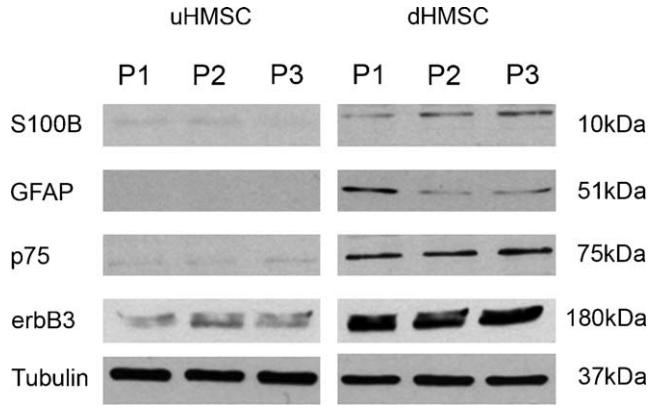

Fig. 7. Expression of glial marker proteins. Western blot analysis of glial cell marker proteins: S100, GFAP, p75, erbB3 in cultured uhMSC and dhMSC for three patients P1–P3. The constitutively expressed beta tubulin protein was used as a positive loading control.

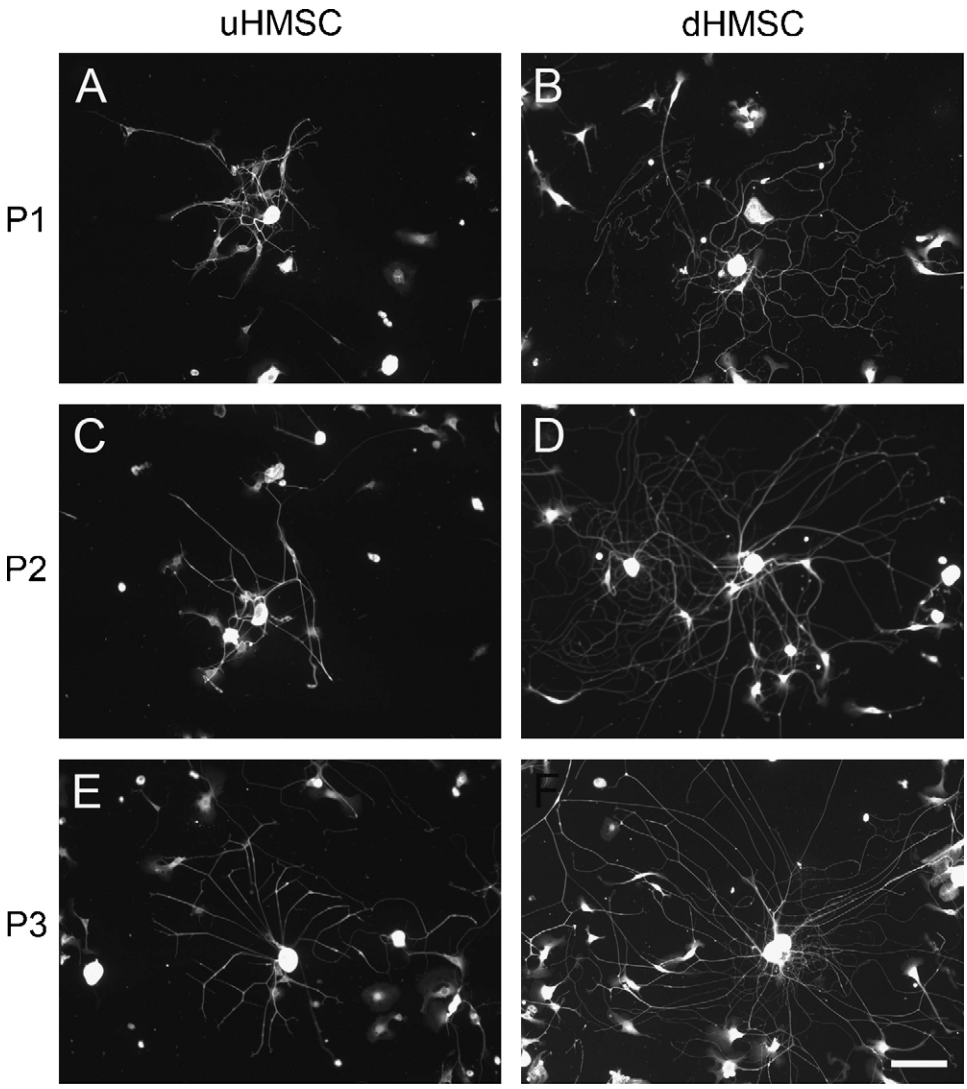

Fig. 8. DRG neurons co-cultured with uhMSC and dhMSC. Immunocytochemical staining for βIII tubulin (Cy3) to show neurites sprouting from DRG neurons following co-culture for 24 h with uhMSC (A, C and E) and dhMSC (B, D and E) from three patients, P1 (A and B), P2 (C and D) and P3 (E and F). Scale bar, 100 μm (A–F).

spond to an effective glial cell differentiation, hence the dhMSC can be functionally interchangeable with SC.

Previous studies have shown that hMSC are capable of supporting regenerating axons in a sciatic nerve injury model in suitably immunosuppressed rats (Shimizu et al., 2007). Our study investigates both the molecular and functional characteristics of hMSC. The hMSC were isolated from three healthy human donors and their cellular identity was verified by their fibroblastic morphology and confirmation of the expression of MSC-specific cell surface markers, Stro-1, CD44, CD54 and CD90 and negative for CD14 and CD45 (Pittenger et al., 1999; Zhou et al., 2005). The multilineage potential of these cells was further evidenced by their ability to undergo differentiation into a variety of cell types (Pittenger et al., 1999; Krampera et al., 2007).

The morphological changes were clearly evident within 4–5 days of culture in the presence of GGF-2; the induction process was similar to that used and seen in rat studies (data not shown). After induction along a glial lineage for 2 weeks, the dhMSC displayed a bipolar, elongated spindle-shape, which is characteristic of SC spindle-like morphology.

In addition to the obvious morphological changes, dhMSC showed a similar to SC pattern and level of expression of glial cell markers. Importantly, this was true for the cells derived from three different patients. Whereas, similar to the rat uMSC, the uhMSC did not express any of the glial markers (Caddick et al., 2006). Specifically, we showed that dhMSC express glial markers p75, GFAP, S100 and the GGF-2 receptor, erbB3 at both the transcriptional and translational level. Although we did not compare the glial marker expression profile of the dhMSC with that of human SC in the present study, it is well known that human SC readily express the standard glial markers such as S100 and GFAP (Bianchini et al., 1992; Mosahebi et al., 2001; Gonzalez-Martinez et al., 2003). There is also no reason to believe that the expression profile of rat SC is markedly different from that of human SC.

In both the rat (Caddick et al., 2006) and human cell co-culture systems, the dMSC promote significantly more neurite outgrowth than do the precursor uMSC. We propose that this increase in neurite outgrowth is the result of the secretion of neurotrophic factors, such as NGF and BDNF, by the hMSC as previously demonstrated for dMSC of rat origin (Mahay et al., 2008b). In order to show that differentiation of hMSC along a glial lineage does not affect the viability of the cells, the proliferation rate of the dhMSC was compared to that of uhMSC. The proliferation rate of the dhMSC was found to be greater than that of the uhMSC. However, this increase may be a response to the presence of SC proliferative

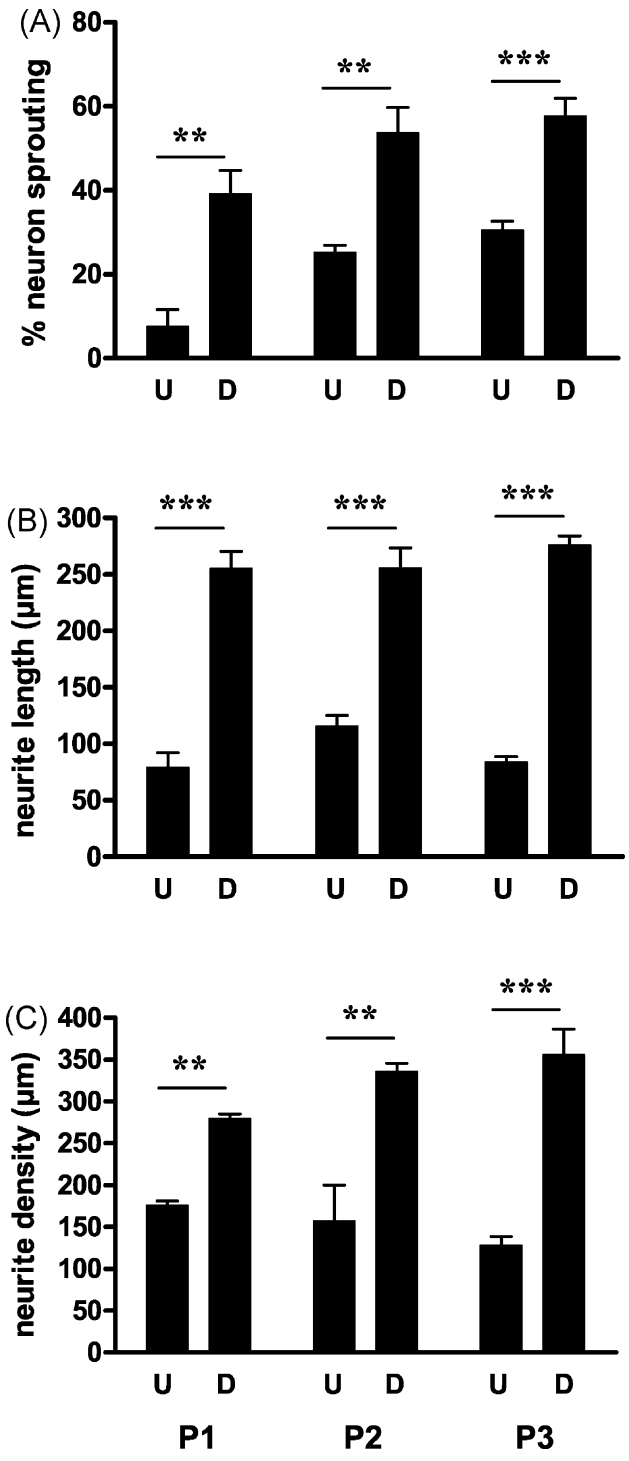

Fig. 9. DRG neuron co-culture quantification. Quantification of neurite outgrowth from DRG neuron following co-culture for 24 h with hMSC for three patients (P1–P3). The percentage of neurons sprouting neurites (A), length of longest neurite (B) and total neurite density (C) were assessed for the uhMSC (U) and dhMSC (D). $^{**}p < 0.01$ and $^{***}p < 0.001$. Error bars show ±S.E.M.

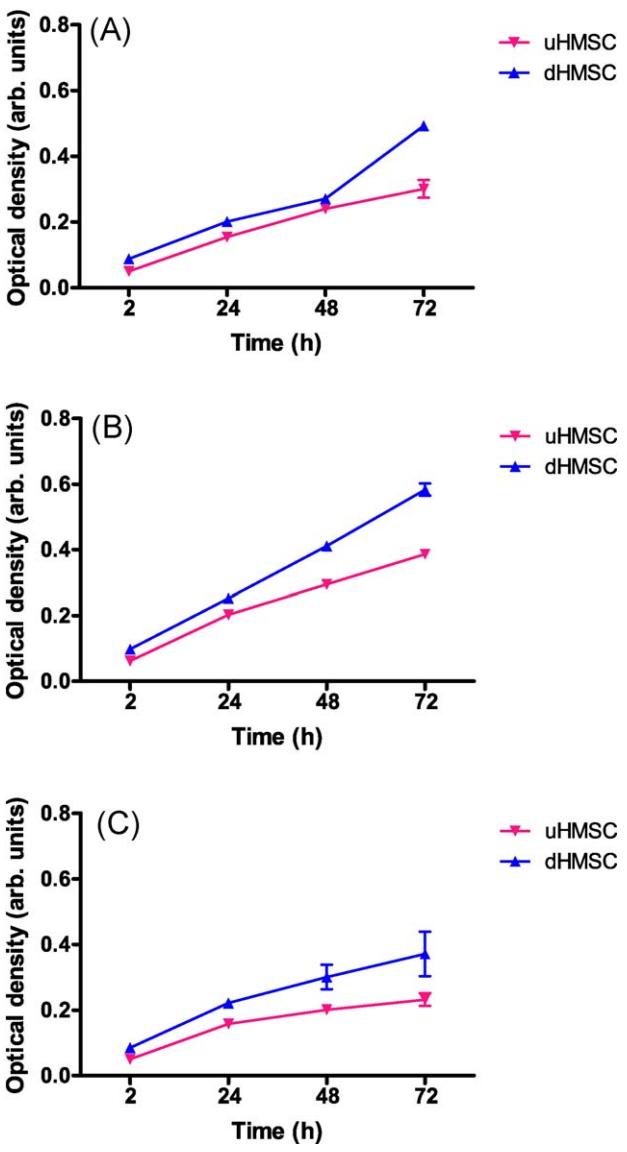

Fig. 10. A comparison of the proliferation rates of uhMSC and dhMSC. For each graph, the lines show the proliferation of pure culture of uHMSC and dHMSC for a given patient over 72 h. In all three patients, the differentiated mesenchymal stem cells show a better rate of proliferation than the undifferentiated stem cells ($p < 0.001$). Error bars show ±S.E.M.

factors, such as bFGF, in the growth medium rather than as a result of the differentiation process *per se* (Go et al., 2007).

Many studies have speculated that the number of MSC within the bone marrow and their differentiation capacity declines with age (Sethe et al., 2006). It has been noted the adult stem cells do suffer the effects of aging *in vivo* resulting in decreased ability to self-renew and properly differentiate (Roobrouck et al., 2008). Aging is thought to be determined by chromosome telomere shortening following cell division; it is well known that cells can escape this process *in vitro* by acquiring mutations in specific genes. It has been reported that telomere length is significantly greater in MSC from young donors than in their older counterparts (Baxter et al., 2004). In addition, telomere length decreases with increase in passage number *in vitro*. Interestingly, there were no qualitative differences in glial marker expression profiles with donor ages of 59, 58 and 32 years old (P1, P2 and P3, respectively). However, a more detailed, quantitative assessment of glial marker expression and molecular characterisation on a larger group of donors of different age and gender is needed before these cells can be regarded as identical. *In vitro*, hMSC have been shown to stop proliferating at passage 40 (Bruder et al., 1997). This is accompanied by an increase in cell size, which is often associated with senescence. In the present study, the hMSC were cultured to passage 10 without any notable changes in their morphology.

The findings of this study provide evidence that human MSC could be differentiated along a glial lineage (dhMSC), express glial cell markers and have functional characteristics similar to those of

SC. As a result of changes in gene expression, the dhMSC are able to function in such a way that they can support significant neurite outgrowth *in vitro* and, therefore, could be used as a SC substitutes to promote peripheral nerve regeneration in clinical applications.

Acknowledgments

This study was supported by the Rosetrees Trust, Medical Research Council (UK), Swedish Medical Research Council, Umeå University, County of Västerbotten, Åke Wibergs Stiftelse, Magn. Bergvalls Stiftelse, Clas Groschinskys Minnesfond, Anna-Stina och John Mattsons Minnesstiftelse för sonen Johan and the Gunvor and Josef Anér Foundation. The authors also wish to thank Acorda Therapeutics for their generous gift of GGF-2.

References

Azizi, S.A., Stokes, D., Augelli, B.J., DiGirolamo, C., Prockop, D.J., 1998. Engraftment and migration of human bone marrow stromal cells implanted in the brains of albino rats—similarities to astrocyte grafts. Proc. Natl. Acad. Sci. U.S.A. 95, 3908–3913.

Barry, F.P., 2003. Biology and clinical applications of mesenchymal stem cells. Birth Defects Res. C: Embryo Today 69, 250–256.

Baxter, M.A., Wynn, R.F., Jowitt, S.N., Wraith, J.E., Fairbairn, L.J., Bellantuono, I., 2004. Study of telomere length reveals rapid aging of human marrow stromal cells following in vitro expansion. Stem Cells 22, 675–682.

Bianchini, D., De, M.I., Cadoni, A., Zicca, A., Tabaton, M., Schenone, A., Anfosso, S., kkad Wattar, A.S., Zaccheo, D., Mancardi, G.L., 1992. GFAP expression of human Schwann cells in tissue culture. Brain Res. 570, 209–217.

Bobis, S., Jarocha, D., Majka, M., 2006. Mesenchymal stem cells: characteristics and clinical applications. Folia Histochem. Cytobiol. 44, 215–230.

Bovetti, S., De, M.S., Gambarotta, G., Fasolo, A., Perroteau, I., Puche, A.C., Bovolin, P., 2006. Differential expression of neuregulins and their receptors in the olfactory bulb layers of the developing mouse. Brain Res. 1077, 37–47.

Bruder, S.P., Jaiswal, N., Haynesworth, S.E., 1997. Growth kinetics, self-renewal, and the osteogenic potential of purified human mesenchymal stem cells during extensive subcultivation and following cryopreservation. J. Cell Biochem. 64, 278–294.

Bunge, R.P., 1994. The role of the Schwann cell in trophic support and regeneration. J. Neurol. 242, S19–S21.

Caddick, J., Kingham, P.J., Gardiner, N.J., Wiberg, M., Terenghi, G., 2006. Phenotypic and functional characteristics of mesenchymal stem cells differentiated along a Schwann cell lineage. Glia 54, 840–849.

Dezawa, M., Takahashi, I., Esaki, M., Takano, M., Sawada, H., 2001. Sciatic nerve regeneration in rats induced by transplantation of in vitro differentiated bone-marrow stromal cells. Eur. J. Neurosci. 14, 1771–1776.

Go, M.J., Takenaka, C., Ohgushi, H., 2007. Effect of forced expression of basic fibroblast growth factor in human bone marrow-derived mesenchymal stromal cells. J. Biochem. 142, 741–748.

Gonzalez-Martinez, T., Perez-Pinera, P., az-Esnal, B., Vega, J.A., 2003. S-100 proteins in the human peripheral nervous system. Microsc. Res. Tech. 60, 633–638.

Harada, T., Harada, C., Mitamura, Y., Akazawa, C., Ohtsuka, K., Ohno, S., Takeuchi, S., Wada, K., 2002. Neurotrophic factor receptors in epiretinal membranes after human diabetic retinopathy. Diabetes Care 25, 1060–1065.

Hofstetter, C.P., Schwarz, E.J., Hess, D., Widenfalk, J., El, M.A., Prockop, D.J., Olson, L., 2002. Marrow stromal cells form guiding strands in the injured spinal cord and promote recovery. Proc. Natl. Acad. Sci. U.S.A. 99, 2199–2204.

Ide, C., 1996. Peripheral nerve regeneration. Neurosci. Res. 25, 101–121.

Keilhoff, G., Goihl, A., Stang, F., Wolf, G., Fansa, H., 2006. Peripheral nerve tissue engineering: autologous Schwann cells vs. transdifferentiated mesenchymal stem cells. Tissue Eng. 12, 1451–1465.

Krampera, M., Marconi, S., Pasini, A., Galie, M., Rigotti, G., Mosna, F., Tinelli, M., Lovato, L., Anghileri, E., Andreini, A., Pizzolo, G., Sbarbati, A., Bonetti, B., 2007. Induction of neural-like differentiation in human mesenchymal stem cells derived from bone marrow, fat, spleen and thymus. Bone 40, 382–390.

Lin, W., Chen, X., Wang, X., Liu, J., Gu, X., 2008. Adult rat bone marrow stromal cells differentiate into Schwann cell-like cells in vitro. In Vitro Cell Dev. Biol. Anim. 44, 31–40.

Mahanthappa, N.K., Anton, E.S., Matthew, W.D., 1996. Glial growth factor 2, a soluble neuregulin, directly increases Schwann cell motility and indirectly promotes neurite outgrowth. J. Neurosci. 16, 4673–4683.

Mahay, D., Terenghi, G., Shawcross, S.G., 2008a. Growth factors in mesenchymal stem cells following glial cell differentiation. Biotechnol. Appl. Biochem. 51, 167–176.

Mahay, D., Terenghi, G., Shawcross, S.G., 2008b. Schwann cell mediated trophic effects by differentiated mesenchymal stem cells. Exp. Cell Res. 314, 2692–2701.

Mosahebi, A., Fuller, P., Wiberg, M., Terenghi, G., 2002. Effect of allogeneic Schwann cell transplantation on peripheral nerve regeneration. Exp. Neurol. 173, 213–223.

Mosahebi, A., Woodward, B., Wiberg, M., Martin, R., Terenghi, G., 2001. Retroviral labeling of Schwann cells: in vitro characterization and in vivo transplantation to improve peripheral nerve regeneration. Glia 34, 8–17.

Pfister, L.A., Papaloizos, M., Merkle, H.P., Gander, B., 2007. Nerve conduits and growth factor delivery in peripheral nerve repair. J. Peripher. Nerv. Syst. 12, 65–82.

Phinney, D.G., 2007. Biochemical heterogeneity of mesenchymal stem cell populations: clues to their therapeutic efficacy. Cell Cycle 6, 2884–2889.

Pittenger, M.F., Mackay, A.M., Beck, S.C., Jaiswal, R.K., Douglas, R., Mosca, J.D., Moorman, M.A., Simonetti, D.W., Craig, S., Marshak, D.R., 1999. Multilineage potential of adult human mesenchymal stem cells. Science 284, 143–147.

Roobrouck, V.D., Ulloa-Montoya, F., Verfaillie, C.M., 2008. Self-renewal and differentiation capacity of young and aged stem cells. Exp. Cell Res. 314, 1937–1944.

Sethe, S., Scutt, A., Stolzing, A., 2006. Aging of mesenchymal stem cells. Ageing Res. Rev. 5, 91–116.

Shimizu, S., Kitada, M., Ishikawa, H., Itokazu, Y., Wakao, S., Dezawa, M., 2007. Peripheral nerve regeneration by the in vitro differentiated-human bone marrow stromal cells with Schwann cell property. Biochem. Biophys. Res. Commun. 359, 915–920.

Terenghi, G., 1999. Peripheral nerve regeneration and neurotrophic factors. J. Anat. 194, 1–14.

Tohill, M., Mantovani, C., Wiberg, M., Terenghi, G., 2004. Rat bone marrow mesenchymal stem cells express glial markers and stimulate nerve regeneration. Neurosci. Lett. 362, 200–203.

Tricarico, C., Pinzani, P., Bianchi, S., Paglierani, M., Distante, V., Pazzagli, M., Bustin, S.A., Orlando, C., 2002. Quantitative real-time reverse transcription polymerase chain reaction: normalization to rRNA or single housekeeping genes is inappropriate for human tissue biopsies. Anal. Biochem. 309, 293–300.

Wiberg, M., Terenghi, G., 2003. Will it be possible to produce peripheral nerves? Surg. Technol. Int. 11, 303–310.

Zhou, Z., Jiang, E.L., Wang, M., Liu, Q.G., Zhai, W.J., Huang, Y., Wang, H.H., Han, M.Z., 2005. Comparative study on various subpopulations in mesenchymal stem cells of adult bone marrow. Zhongguo Shi Yan Xue Ye Xue Za Zhi 13, 54–58.

Zurita, M., Bonilla, C., Otero, L., Aguayo, C., Vaquero, J., 2008. Neural transdifferentiation of bone marrow stromal cells obtained by chemical agents is a short-time reversible phenomenon. Neurosci. Res. 60, 275–280.

Zurita, M., Vaquero, J., Oya, S., Bonilla, C., Aguayo, C., 2007. Neurotrophic Schwann-cell factors induce neural differentiation of bone marrow stromal cells. Neuroreport 18, 1713–1717.